Investigation of Vortex Introducing Severe Flow Accelerated Corrosion in A Loop System

Siqiao FENG[1], Changfeng CHEN[1]

[1] Beijing Key Laboratory of Failure, Corrosion and Protection of Oil/gas Facilities, Department of Materials Science and Engineering, China University of Petroleum (Beijing), China PR

Abstract

Flow accelerated corrosion is typical corrosion phenomena in the oil and gas industry. The effect of the vortex on flow accelerated corrosion was investigated in this research. To simulate the oil and gas field, a loop flow system and Fluent simulation software were used. The results show that in loop corrosion system a higher corrosion rate was gained in 3% NaCl solution with 0.3MPa CO_2 pressures and different flow rate(0.25m/s, 0.4m/s and 0.5m/s) than in the autoclave. The corrosion products morphology on the coupons surface in the loop corrosion system was smooth, with the flake-shape corrosion product falling in some areas. Fluent simulation results show that the vortex was the main reason for flow accelerated corrosion. In the complete turbulence condition, vortices were formed in the transitional layer from laminar to turbulent, transferring Fe^{2+} from viscous sublayer to the bulk fluid. The movement of Fe^{2+} to the bulk solution increased the dissolution rate of corrosion products on the surface. Thus, the corrosion was accelerated as the flow rate increased. The viscous sublayer became thinner, while the vortex strength near the wall gradually increased, which made severe corrosion on the sample surface.

Keywords: flow accelerated corrosion; vortex; complete turbulence; simulation

Introduction

Flow accelerated corrosion(FAC) refers to the phenomenon of accelerated metal destruction caused by the relative movement between the corrosive fluid and the metal surface, which is usually caused by the synergistic action of fluid flushing and corrosion [1]. According to different corrosive media, it can be divided into single-phase FAC, double-phase FAC and multi-phase FAC. However, the most studied are liquid-gas and liquid-solid double-phase FAC. Currently, the theory of FAC is not perfect [2,3].

In 1990, Prof. U.Lotz and J.Postlethwaite of Canada adopted the principle of conservation of axial and radial momentum based on the continuity equations and conservation of mass in fluid dynamics. The experimental equipment of the loop corrosion system was established to study the flow pattern changes of sudden contraction and sudden expansion of the pipe section for the first time. It is preliminarily believed that the abrupt changes in pipe geometry can lead to the formation of different sizes vortices during fluid flow. The formation of this vortices is the main cause of accelerated corrosion [4]. In the late

1990s, the loop flow accelerated corrosion only stayed in the software simulation stage. Ma,K.T.,Ferng,Y.M. and Ma,Y.P. used fluent software to simulate the liquid-gas double-phase flow in the pipeline, indicating that the degree of corrosion is different at each position of the bent pipe section during the flow [5]. In 2010, M.El-Gammal simulated the effect of fluid hydraulic action on the FAC process. The results show that the impact of the fluid will make the wall thickness thinner [6]. It was not until 2011-2015 that researchers were able to combine fluid flow regimes with electrochemical corrosion by experimental means for validate the simulation results, and then the factors that influence the FAC are systematically analyze [7-10].

Compared with the conventional high-temperature and high-pressure autoclave, the loop corrosion system is more similar to the actual corrosion of oil pipelines. In the autoclave, corrosive sample drives the corrosion solution to rotate, a relatively low flow rate is generated between the corrosion sample and the corrosion solution, which is dominated by the mass transfer process in its corrosion process (Fig.1) [11]. In this state, the dissolution and diffusion rate of corrosion products is slower, the protective effect on the metal surface is better and the corrosion rate is lower; while the corrosion rate between the fixed corrosion sample and the flowing corrosion solution in the loop corrosion system has a relatively high flow rate. As the flow rate increases, the corrosion process gradually transitions from reaction control to FAC control (Fig.1) [12,13]. At higher flow rates, the rate of wall thinning increases, and which is affected by three stages: 1) The rate of electrochemical oxidation to produce Fe^{2+} on the metal surface; 2) The deposition rate of Fe^{2+} on the metal surface and the dissolution rate of the outermost corrosion products in the boundary layer electrolyte; 3) The diffusion rate of Fe^{2+} from the boundary layer to the bulk fluid; As the flow rate increases, the mass transfer rate at the boundary layer increases, accelerating the dissolution rate of the corrosion products on the metal surface and the diffusion rate to the bulk fluid, thereby promoting the thinning of the wall, causing a sharply corrosion rate [14-17].

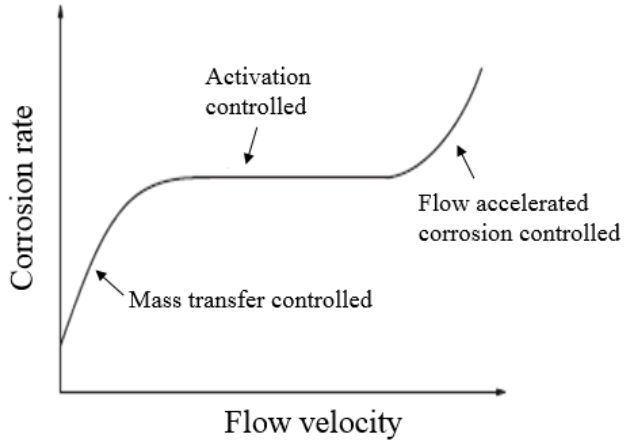

Fig.1. Corrosion control process

The corrosion of L360 carbon steel in the loop corrosion system and the autoclave at different flow rates in 0.3MPa CO_2 of 3% sodium chloride was studied. It was found that the corrosion rate of the L360 carbon steel using the loop corrosion system test under the same conditions was 1.5 times that of the autoclave. The corrosion product morphology on the

sample surface in the loop system was smooth, with the flake-shape corrosion product falling in some areas. Fluent simulation results show that the vortex was the main reason for flow accelerated corrosion. In the complete turbulence condition, vortices were formed in the transitional layer from laminar to turbulent, transferring Fe^{2+} from viscous sublayer to the bulk fluid, further promote the dissolution of corrosion products on the metal surface and accelerate wall thinning.

Experimental

Loop corrosion system

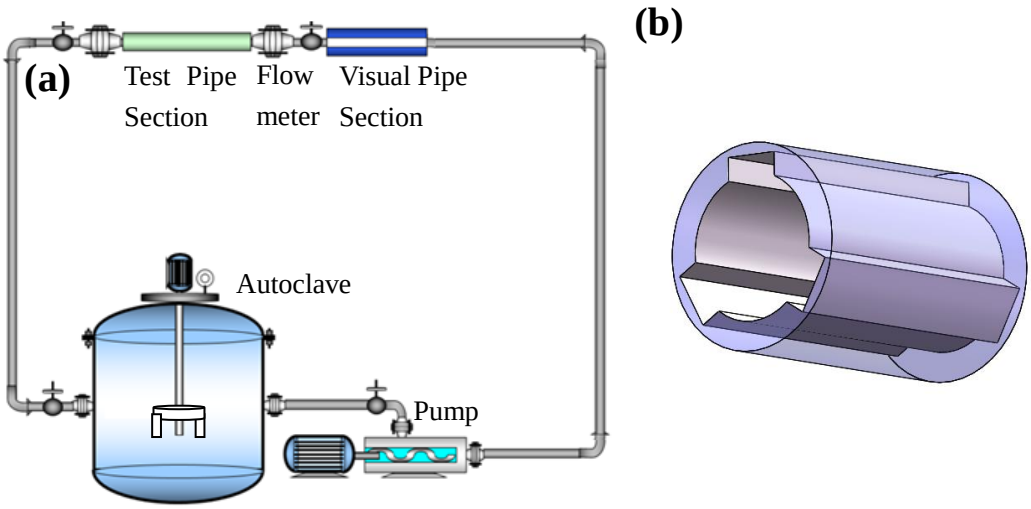

Fig.2. Schematic diagram of flow accelerated corrosion loop corrosion system and corrosion sample mold: (a) loop corrosion system, (b) corrosion sample mold

Loop corrosion system experimental equipment consists of five parts: high temperature and high pressure autoclave, pump, visual pipe section, test pipe section and flow meter (Fig.2(a)). The autoclave is mainly used for containing corrosive liquids and controlling the temperature of corrosive liquids. Suspension corrosion coupons can be placed in the autoclave for corrosion experiment. The autoclave is connected with the entire loop pipe section, and the gas is introduced into the solution through the autoclave to maintain a constant pressure in loop corrosion system during experiment. The pump can change the flow rate of the fluid in loop corrosion system and determine the flow rate value through flow meter. Placing a mold which embedded the coupons in the test pipe section for FAC test, FAC mold was made of teflon, each mold can be embedded with three FAC coupons (fig.2(b)). Six molds can be placed in the test pipe section for parallel testing and the flow pattern can be observed under different flow patterns of the fluid flow rate through visual pipe section during the test.

Materials and corrosion environment

Pipeline carbon steel (L360) coupons, with the chemical composition of 97.6% Fe, 0.16% C, 1.6% Mn, 0.45% Si, 0.015% S, 0.025% P, 0.06%V, 0.05%Nb and 0.04%Ti, were cut with dimensions of 50mm ×10 mm ×3 mm from a pipeline sample,

All coupons were ground with 400, 800, 1200 and 1500 grit silicon carbide paper, and finally polished with W2.5 diamond polishing paste. The polished coupons was cleaned with acetone and then dried under warm air. Vernier caliper was used to measure the exact size of the corroded specimen to determine the corrosion rate. A 6mm hole was punched in one end of the partially cut coupons, using teflon screws to fix it on the teflon rotating plate in the autoclave to perform corrosion experiments. The coupons in loop corrosion test section was sealed with 704 silicone rubber on 5 sides, and the sealed coupons was embedded in mold so that only a 50 mm x 10 mm surface was left for each test coupons to carry out the loop corrosion test.

The corrosive liquid in the corrosive environment is mainly composed of 3% sodium chloride solution, and total volume of the solution is 30L, the entire loop corrosion system is deoxygenated by passing N_2 through the autoclave for 15 hours, a 0.3 MPa CO2 corrosive gas was introduced and the corrosion solution temperature was maintained at 50℃ for the corrosion test.

Characterization of corrosion products after corrosion

After corrosion test in loop corrosion system, the corrosive coupons in the autoclave and loop test pipe sections were taken out and soaked in an acetone solution for dehydration, and then dried under warm air. The surface morphology of the corrosion product was observed under a scanning electron microscope (SEM) and the composition of the surface corrosion product was determined by X-ray diffraction (XRD).

Weight loss and corrosion rate analysis

The corrosion rate of coupons was calculated by measuring the corrosion weight loss of corrosion coupons. The corrosion coupons in autoclave and loop corrosion system were immersed in 10% hydrochloric acid solution while adding a small amount of hexamethylenetetramine protected metal substrate, after washing for 5 to 10 minutes under ultrasound, the surface hydrochloric acid solution was washed with deionized water, the 704 silicone rubber covered by the surface of the coupons in the loop corrosion system was scraped with a blade, dehydrated in an acetone solution, and then weighing after dried under warm air.

The formula for calculating the uniform corrosion rate of corrosion coupons in autoclave and loop corrosion system is as follows[18]:

$$\text{Corrosion rate}(\text{mm}/\text{a})=\frac{8.76\times10^{4}\times\text{weight loss}(\text{g})}{\text{density}(\text{g}/\text{cm}^{3})\times\text{area}(\text{cm}^{2})\times\text{time}(\text{h})}$$

The calculation of the coupons surface area in the formula is very important. Coupons in the autoclave need to calculate the area of all the surface areas to remove the two round holes, while the corrosion coupons in loop corrosion system only needs to calculate the surface area of one etched surface.

Numerical simulation

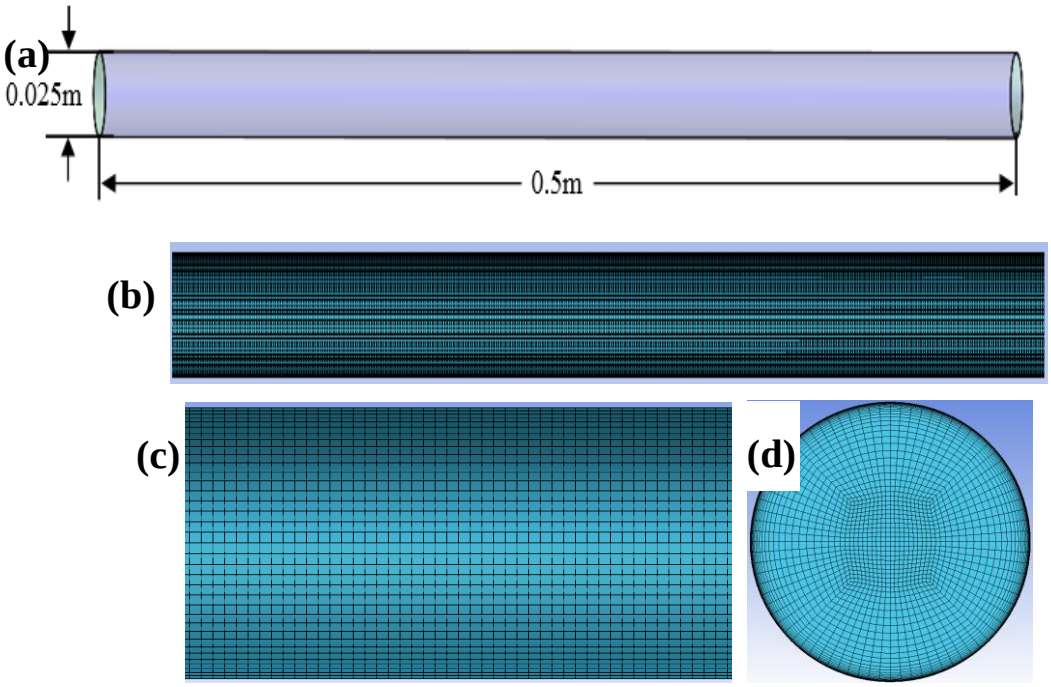

Fig.3. Schematic diagram of pipeline model and meshing: (a) three-dimensional solid model, (b)meshing, (c) partial enlarged grid, (d) section meshing

Build a three-dimensional solid model with a diameter of 0.025m and a length of 0.5m by SolidWorks software (Fig.3(a)). Import this solid model into ANSYS Workbench to create a fluid model, and then meshing through the ICEM module in ANSYS, volume meshes were constructed with the max interval size of 0.001m（Fig.3(b) and Fig.3(c) and the total number of grids is 1,382,261. In order to study the flow pattern of the fluid near wall, the mesh near wall surface is encrypted (Fig.3(d)). Set fluid inlet face type to VELOCITY-INLET, outlet face type to OUTFLOW, and wall type to WALL. Fluent fluid simulation software in ANSYS was used to simulate the fluid flow regime, inlet speeds were set to 0.25m/s, 0.5m/s, 1m/s, 1.5m/s, and 2m/s under 0.3MPa simulation pressure, respectively. According to the incompressibility of the fluid, k-e double equation turbulence model was used to simulate the solution, k, which refers to turbulent kinetic energy, was set as $1m^2/s^2$ and e, which refers to turbulent dissipation rate, was set as $1m^2/s^3$. The k–e turbulence equation was solved by iterative method with a convergence criterion of 0.00001 [19-23].

Results

Weight loss measurement

After corrosion test in autoclave and loop corrosion system, it was found that the uniform corrosion rate of L360 was high at a temperature of 50 ℃ and a CO_2 partial pressure of 0.3 MPa. When the flow rate is 0.25m/s, the corrosion rate in loop corrosion system and

autoclave is 15.9mm/a and 9.8mm/a, respectively. The uniform corrosion rate of coupons in loop corrosion system is about 1.5 times than that in autoclave. With the increase of the flow rate, the uniform corrosion rate in loop corrosion system and autoclave significantly increased. When the flow rate increased to 0.5 m/s, the corrosion rate in loop corrosion system and autoclave increased to 23.1 mm/a and 17.6mm/a (Fig.4).

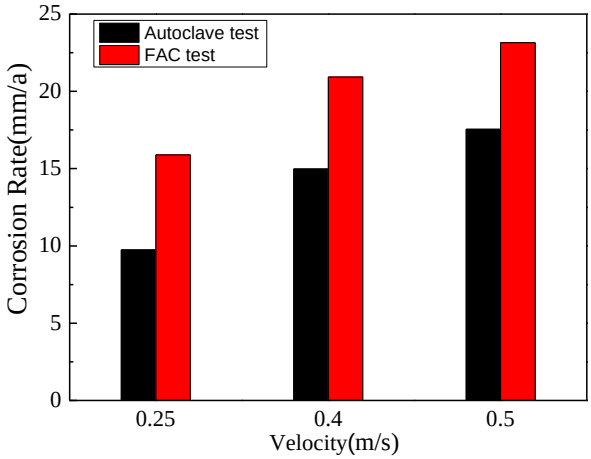

Fig.4 Uniform corrosion rates at different flow rates

Analysis of corrosion products

After corrosion test in loop corrosion system and autoclave, the corrosion products on the surface of coupons was observed by SEM. It was found that the corrosion products on the surface of coupons in autoclave showed a natural growth state. With the increase of the flow rate, the granular corrosion products on the surface of coupons gradually increased, the surface of the corrosion products was rough, and the undulation was large (Fig.5(a), (c) and (e)) [24], Some local areas showed a massive exfoliation, and expose the bottom substrate (Fig.5(c)). However, for corrosion coupons in loop corrosion system, as the flow rate increase, the bond between corrosion products particles on the surface of coupon gradually becomes tighter and the corrosion products surface is smoother with the flake-shape corrosion products falling in some areas (Fig.5(b), (d) and (f)), after flake-shape corrosion products falling the granular corrosion products were still visible at the bottom (Fig.5(d)) [25].

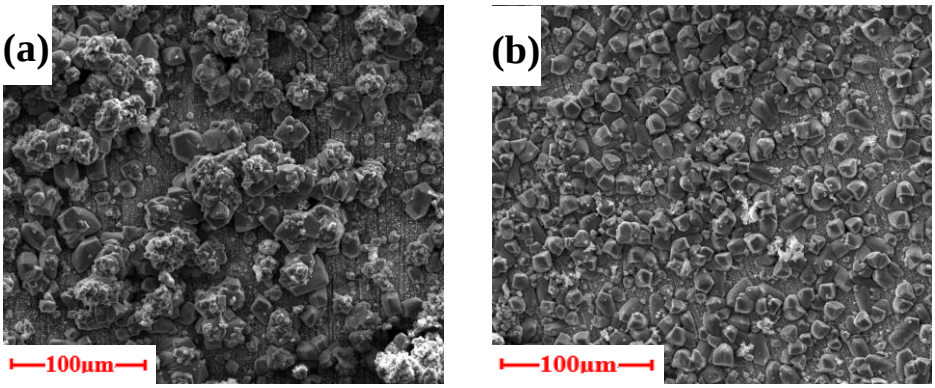

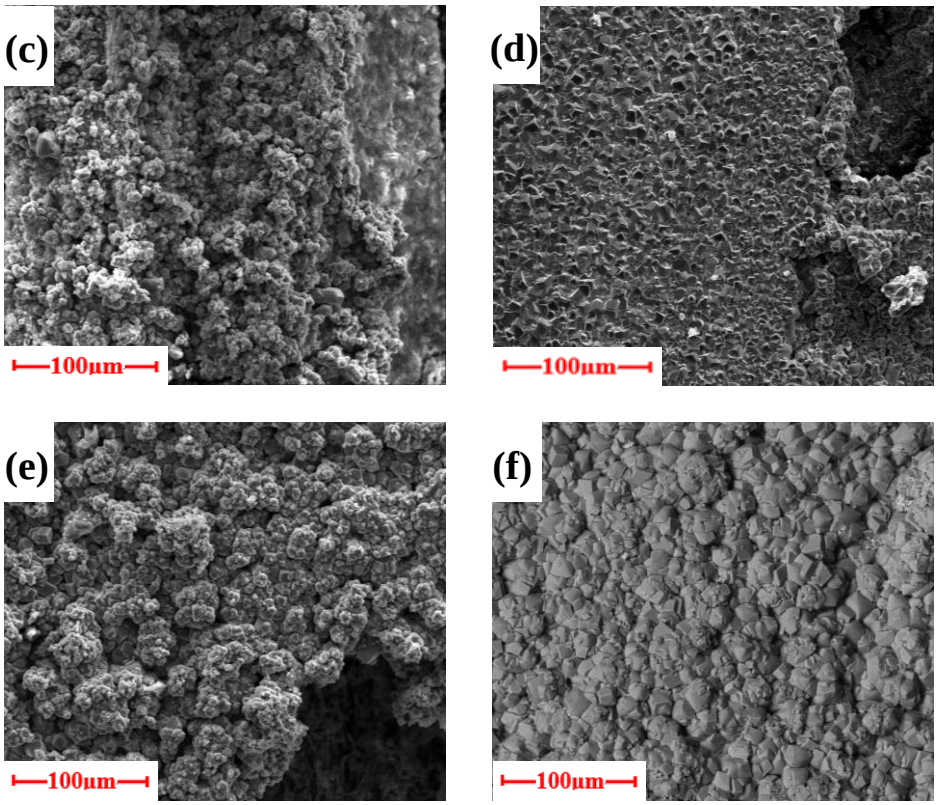

Fig.5 Corrosion products topography in autoclave and loop corrosion system under different flow rates: (a), (c), (e) were 0.25m/s, 0.4m/s, 0.5m/s in autoclave; (b), (d), (f) were 0.25m/s, 0.4m/s, 0.5m/s in loop corrosion system

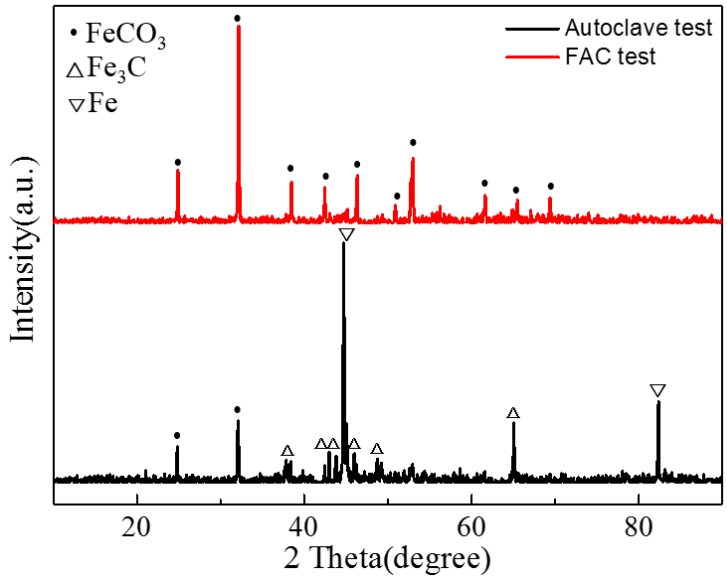

Fig.6 Corrosion coupons XRD analysis results at 0.5m/s flow rate after corrosion in autoclave and loop corrosion system

In order to determine the specific composition of corrosion products on the corrosion surface of the coupons, XRD analysis was performed on corrosion coupons with a flow rate

of 0.5 m/s in autoclave and in loop corrosion system. The results show that the surface of coupons in autoclave contains granular $FeCO_3$ and Fe_3C (Fig.6), among them, $FeCO_3$ is the main corrosion products produced by CO_2 corrosion, and Fe_3C is the exposed cementite after surface block $FeCO_3$ falling[26]; The surface of the coupons corroded in Loop corrosion system contains only a large amount of $FeCO_3$ particles, but the surface $FeCO_3$ with flake-shape falling in some areas and after flake-shape $FeCO_3$ falling the granular $FeCO_3$ were still visible at the bottom (Fig.5(d)).

Fluent simulation

By comparing the corrosion of coupons in autoclave and loop corrosion system, it is found that the surface corrosion morphology is quite different, FAC in loop corrosion system is closer to the corrosion of the oil and gas industry. After obtained the flow pattern of the fluid by Fluent simulation [27,28] the corrosion mechanism of FAC in loop corrosion system is further analyzed.

(1) Velocity distribution

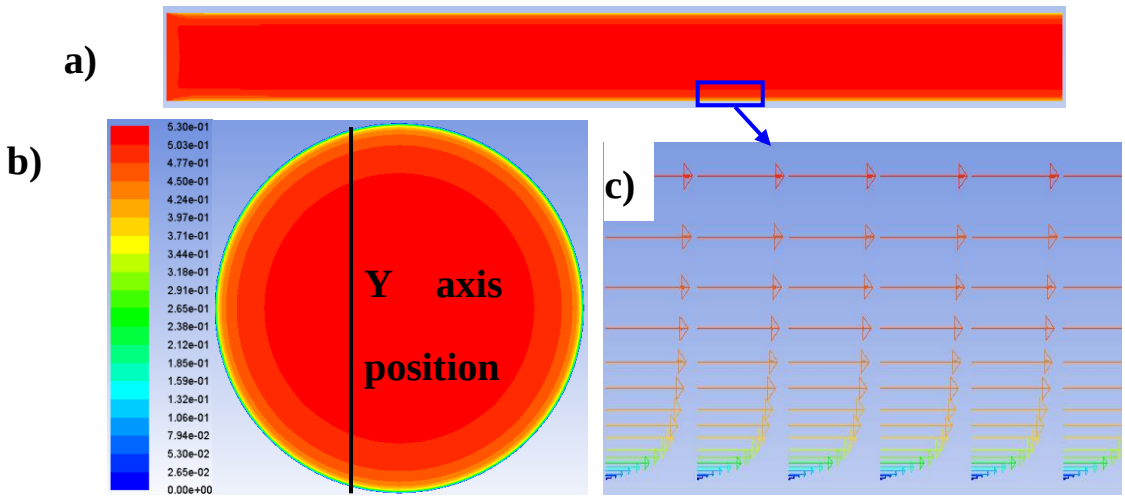

Fig.7 Velocity distribution in pipeline at flow rate of 0.5m/s: (a) integral pipeline flow rate distribution, (b) cross section flow velocity distribution, (c) flow velocity distribution near the wall

In order to determine the flow pattern of the fluid in the pipeline, the speed cloud diagram in the simulation results are analyzed. Fig.7(a) and Fig.7(b) are integral pipeline and cross sectional view of the velocity distribution at a velocity of 0.5 m/s. It can be seen from the figure that the flow pattern of the main fluid in the pipeline is similar, further analysis of the speed vector near the wall surface can be obtained: due to the viscosity of the fluid, there is a certain velocity gradient near the wall surface, and the closer to the wall the velocity is lower.

(2) Vortex intensity near wall

The corrosion solution with a flow rate of 0.25 m/s or more is in a turbulent flow state, and the formation conditions of turbulent flow must form vortices and its movement to critical fluids. It can be seen in Fig.8 that as the flow velocity of the fluid increase, the vortex

intensity at the near wall gradually increase. The greater the velocity gradient between adjacent fluids near the wall, the higher the vortex intensity of the vortex formed[30], and then the vortex near the wall can accelerate the dissolution rate of corrosion products on the metal surface [31].

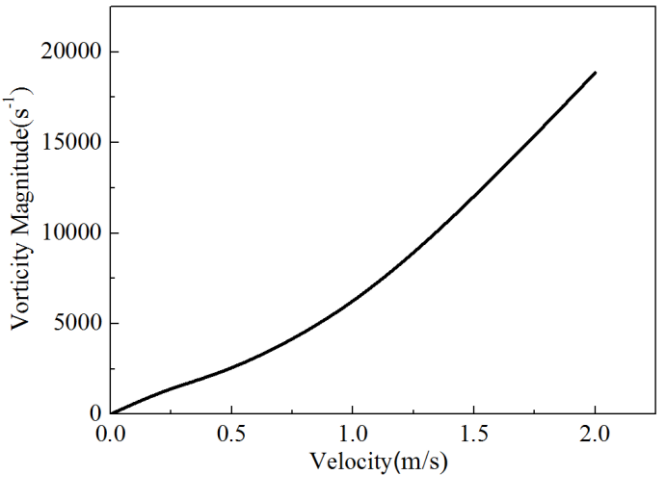

Fig.8 The relationship between flow velocity and vortex intensity near the wall

(3) Turbulence intensity

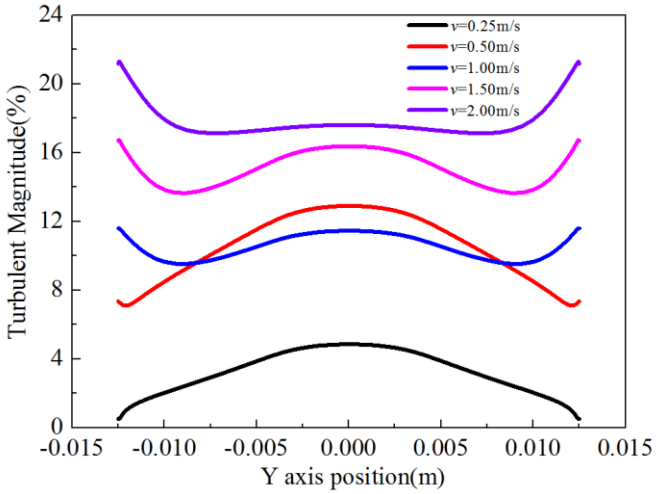

Fig.9 The relationship between flow velocity and turbulence intensity at Y axis position

The turbulent intensity of a fluid is a physical quantity that measures the pulsation degree of a liquid. Therefore, the pulsation degree of a fluid with a large turbulence intensity is large. An increase in the pulsation degree of the fluid can enhance the interaction between the fluid at that location and the critical fluid, thereby enhancing mass transfer and momentum transfer. Select the Y axis position at the cross section of Fig.7(b) to establish the turbulence intensity at different positions on the Y axis position at different flow velocities(Fig.9). It can be seen from the figure, as the flow rate increase, the pulsation at the near wall surface of the fluid increase, and the interaction with the critical fluid increase.

Discussion

By comparing the experimental results of the two experimental devices, it is found that the corrosion rate of coupons in loop corrosion system is higher than that in autoclave, which is similar to the corrosion in the corrosive environment of actual oil and gas field, belongs to FAC. The corrosion mechanism of the FAC is mainly contain: (1) The corrosive liquid forms a vortex near wall surface and generates a higher vortex intensity, accelerating the dissolution of the surface corrosion product; (2) The vortex near wall surface carries the dissolved Fe^{2+} and CO_3^{2-} migrates to the bulk fluid, reducing the corrosion coupons surface Fe^{2+} and CO_3^{2-} concentrations, and then promote exposed metal substrates continue corrosion.

（1）Formation of vortex near wall

The flow pattern of the fluid can be determined based on the Reynolds number (*Re*), and the relationship between Reynolds number and flow rate can be expressed by the following equation:

$$Re = \frac{\rho \bar{u} d}{v}$$

Where ρ is density for metal materials, $\bar{u}$ is velocity, d is feature length and v is fluid viscosity.

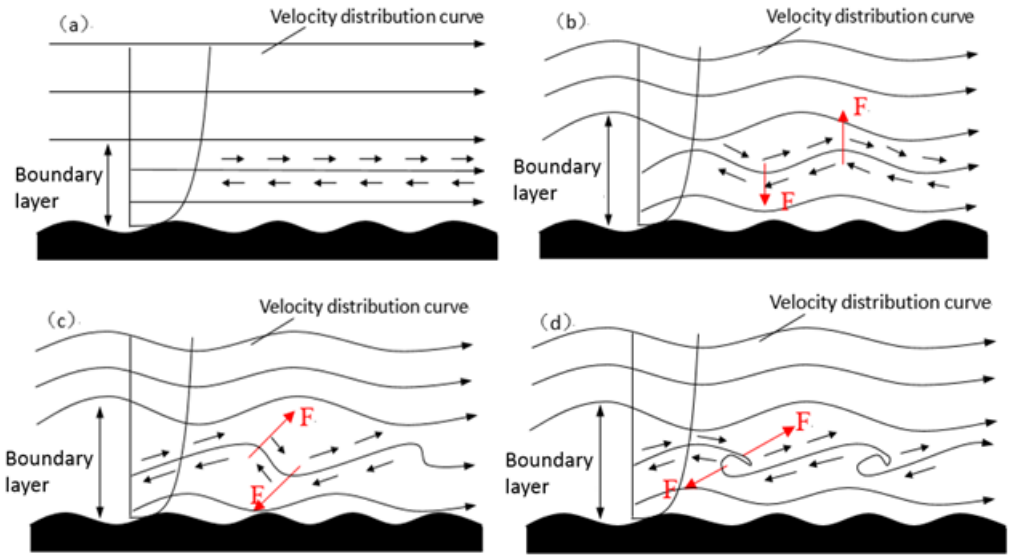

Fig.10 Schematic diagram of vortex formation process

Therefore, the Reynolds number of a corrosive liquid with a flow rate of 0.25m/s in this pipeline Re = 6250, which is greater than 4000 and in a turbulent state [24,29]. Increasing the flow rate will continue to increase the turbulence degree, and the essence of turbulence is the formation and migration of vortices. It can be seen from the formation of the vortex at turbulent boundary layer in Fig.10. Because the fluid has a certain viscosity, the flow velocity in boundary layer is characterized by a gradient distribution. The boundary layer consists of a viscous sublayer near the metal and a transitional layer from laminar to turbulent. The thickness of viscous sublayer and transitional layer gradually becomes thinner as the flow rate increases. For a certain flow layer, a critical flow layer with a velocity greater than that is

applied with a shear stress in the forward direction, and a flow layer near wall with a velocity smaller than that is applied with the shear stress in the reverse flow direction. The opposite direction of shear forces in primary flow layer will constitute moments, and then getting a tendency to form vortex (Fig.10(a)) [30]. However，for flowing fluids, slight turbulent pulsations occur in the transitional layer from laminar to turbulent, the flow velocity is increased and the pressure is decreased due to the reduction of the cross-section of the micro-flow beam at the rise of the flow layer, while the flow velocity is decreased and the pressure is increased at the indentation, stimulate slightly fluctuating fluid layers to withstand a certain lateral pressure (Fig.10(b)), which promotes more drastic fluctuations in the flow zone (Fig.10(c)), under the combined effect of lateral pressure and shear forces, the vortices thus formed (Fig.10(d)), and the magnitude of vortex intensity is related to the gradient of velocity near the wall [32-35].

（2）Effect of vortex movement near the wall on corrosion

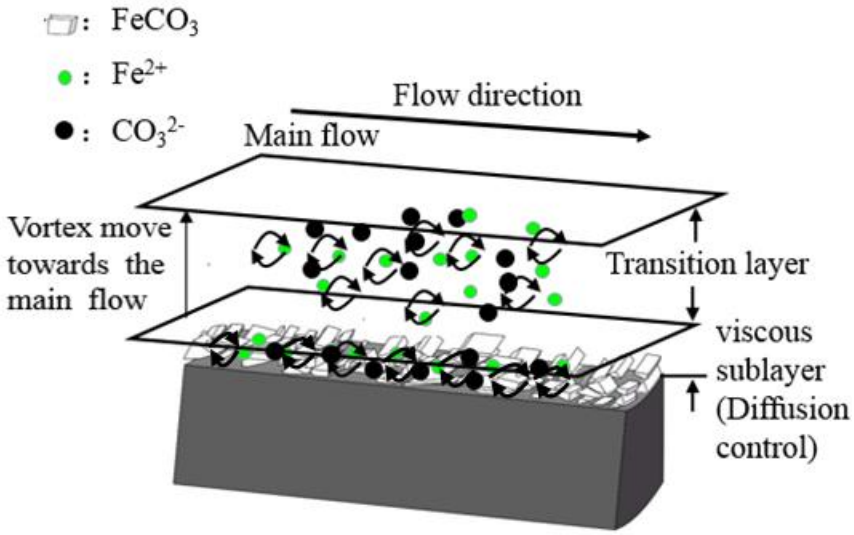

Fig.11 Flow accelerated corrosion mechanism diagram

The vortex intensity of the fluid near wall surface of the viscous sublayer is larger, the swirling rate of the vortex is higher, and the dissolution of surface corrosion products and the diffusion rate of ions into the transition layer are accelerated. When ions diffuse into the transition layer, the intensity of the vortex is only slightly reduced. For a certain vortex, the flow velocity on the side close to the bulk fluid is higher and the pressure is lower, while the flow velocity on the side near the wall is lower and the pressure is higher, and upward lift is generated during the interaction with the fluid, carrying the dissolved corrosion product ions migrates to the critical fluid layer, and gradually diffuses to the bulk fluid. The diffusion rate of the vortex to bulk fluid is related to turbulence intensity, the greater the turbulence intensity is, the more violent the pulsation of the turbulent flow is, the faster the vortex moves from transition layer to bulk fluid, the more severe the corrosion is. The increase of ions transported from transition layer to bulk fluid will reduces the ion concentration in the transition layer, and the concentration difference between dissolved corrosion product ions in viscous sublayer and transition layer becomes larger, accelerating the diffusion rate of ions in the viscous

sublayer, which in turn promoting the dissolution of corrosion products on the metal surface. Long-term FAC can lead to thinner walls.

Conclusions

Corrosion test of autoclave and loop corrosion system under the same conditions found that the corrosion rate in loop corrosion system was about 1.5 times than that in autoclave. The corrosion products on the surface of coupons in autoclave showed a natural growth state, that made the surface rough; However, the corrosion products morphology on the coupons surface in the loop corrosion system was smooth, which is similar to the FAC during oil and gas field production. Further simulation revealed that the vortexes in viscous sublayer and the transition layer are the main causes of FAC. The vortex in viscous sublayer can accelerate the dissolution of surface corrosion products and the diffusion rate of ions into the transition layer, the vortices in transition layer generate a lift to bulk fluid under the effect of turbulent pulsation, and carrying the dissolved corrosion product ions into the bulk fluid, the more ions migrated from transition layer to bulk fluid, the lower the ion concentration in transition layer, so that the concentration difference between dissolved corrosion product ions in viscous sublayer and transition layer becomes larger, accelerating the diffusion rate of ions in the viscous sublayer, which in turn promoting the dissolution of corrosion products on the metal surface. Therefore, in the oil and gas field production process, long-term FAC will lead to thinning of the pipe wall.

References

1. Subir Paul, Anjan Pattanayak, and Sujit K. Guchhait, Corrosion Behavior of Carbon Steel in Synthetically Produced Oil Field Seawater, 2014(2014), pp.1-11.

2. Benedetto Bozzini, Marco E. Ricotti, Marco Boniardi, Claudio Mele, Evaluation of Erosion-corrosion in Multiphase Flow via CFD and Experimental Analysis, Wear, 255(2003), pp. 237-245.

3. Songying Chen, Junjie Mao, Deposition of Chloride in Two-phase Flow for the Superheater via Numerical Simulation, Advanced Materials Research, 354(2011), pp.236-239.

4. Lotz U, Postlethwaite J. Erosion-corrosion in Disturbed Two Phase Liquid/particle Flow, Corrosion Science, 30(1990), pp.95.

5. Ma K T, Ferng Y M, Ma Y P, Numerically Investigating the Influence of Local Flow Behaviors on Flow-Accelerated Corrosion Using Two-Fluid Equations, Nuclear Technology, 123(1998), pp.90-102.

6. El-Gammal M, Mazhar H, Cotton J S, et al, The hydrodynamic effects of single-phase flow on flow accelerated corrosion in a 90-degree elbow, Nuclear Engineering & Design, 240(2010), pp.1589-1598.

7. L. Zeng, G.A. Zhang, X.P. Guo. A Study of Flow Accelerated Corrosion at Elbow of Carbon Steel Pipeline by Array Electrode and Computational Fluid Dynamics Simulation, Corrosion Science, 77(2013), pp.334-341.

8. L. Zeng, G.A. Zhang, X.P. Guo. Erosion‐corrosion at Different Locations of X65 Carbon Steel Elbow, Corrosion Science, 85(2014), pp.318-330.

9. H.P. Rani, T. Divya, R.R. Sahaya, Vivekanand Kain, D.K. Barua. CFD Study of Flow Accelerated Corrosion in 3D Elbows. Annals of Nuclear Energy, 69(2014), pp.344-351.
10. X.L.Zhu, X.F.Lu, and X.Ling, A Novel Method to Determine the Flow Accelerated Corrosion Rate in the Elbow, Materials and Corrosion, 64(2013), pp.486-492.
11. Evgeny Barmatov, Trevor Hughes, Michaela Nagl, Efficiency of Film-forming Corrosion Inhibitors in Strong Hydrochloric Acid under Laminar and Turbulent Flow Conditions, Corrosion Science, 92(2015), pp.85-94.
12. John M. PIETRALIK, The Role of Flow in Flow-accelerated Corrosion under Nuclear Power Plant Conditions, E-Journal of Advanced Maintenance, 4(2012), pp.63-78.
13. X.L.Zhu, L.X.Zhu, X.F.Lu, X.Ling, A Novel Method to Determine Flow-accelerated Corrosion Rate Based on Fluid Structure Interaction, Materials and Corrosion, 65(2014), pp.1120-1127.
14. Douglas Munson, A Brief Overview of FAC Investigation, Experiences and Lessons Learned, Seminar on Effective Monitoring and Control of Flow Accelerated Corrosion (FAC), Haiyan, 2007.
15. H. Mazhar, D. Ewing, J.S. Cotton, C.Y. Ching, Experimental Investigation of Mass Transfer in 90° Pipe Bends Using a Dissolvable Wall Technique, International Journal of Heat and Mass Transfer, 65(2013), pp.280-288.
16. Tsuyoshi Takano , Yuya Ikarashi , Kazuya Uchiyama , Takayuki Yamagata , Nobuyuki Fujisawa, Influence of Swirling Flow on Mass and Momentum Transfer Downstream of a Pipe with Elbow and Orifice, International Journal of Heat and Mass Transfer, 92(2016), pp.394-402.
17. Feng Shan , Zhichun Liu , Wei Liu , Yoshiyuki Tsuji, On Flow Structures Associated with Large Wall Mass Transfer Coefficients in Orifice Flows. International Journal of Heat and Mass Transfer, 102(2016), pp.1-9.
18. M.A. Javed, P.R. Stoddart, S.A. Wade, Corrosion of Carbon Steel by Sulphate Reducing Bacteria: Initial Attachment and the Role of Ferrous ions, Corrosion Science, 93(2015), pp.48-57.
19. Zhang G A, Liu D, Li Y Z, et al, Corrosion Behaviour of N80 Carbon Steel in Formation Water under Dynamic Supercritical CO_2 condition, Corrosion Science, 120(2017), pp.107-120.
20. L.W. Li, S. Khorsandi, R.T. Johns, R.M. Dilmore, CO_2 Enhanced Oil Recovery and Storage Using a Gravity-enhanced Process, Int. J. Greenh. Gas Control, 42(2015), pp.502–515.
21. Kazutoshi Fujiwara, Masafumi Domae, Kimitoshi Yoneda, Fumio Inada, Model of Physico-chemical Effect on Flow Accelerated Corrosion in Power Plant, Corrosion Science, 53(2011), pp.3526-3533.
22. Ronald E. Vieira, Mazdak Parsi, Netaji R. Kesana, Siamack A. Shirazi, and Brenton S. McLaury, Effects of Flow Pattern and Flow Orientation on Sand Erosion in Elbows for Multiphase Flow Conditions, Corrosion, 5434(2015), pp.1-15.

23. Quamrul H. Mazumder, Effect of Liquid and Gas Velocities on Magnitude and Location of Maximum Erosion in U-bend, Open Journal of Fluid Dynamics, 2(2012), pp.29-34.
24. Lilian Raquel Moretto Ferreira, Haroldo Araujo Ponte, Luciana Schmidlin Sanches, Ana Carolina Tedeschi Gomes Abrantes, CO_2 Corrosion in the Region Between the Static and Turbulent Flow Regimes, Materials Research, 18(2015), pp.245-249.
25. María Elena Olvera-Martínez, Juan Mendoza-Flores, J. Genesca, CO_2 Corrosion Control in Steel Pipelines. Influence of Turbulent Flow on the Performance of Corrosion Inhibitors, Journal of Loss Prevention in the Process Industries, 35(2015), pp.19-28.
26. J.L. Mora-Mendoza, S. Turgoose, Fe_3C Influence on the Corrosion Rate of Mildsteel in Aqueous CO_2 Systems under Turbulent Flow Conditions, Corrosion Science, 44(2002), pp.1223–1246.
27. R. Elgaddafi, A. Naidu, R. Ahmed, S. Shah, S. Hassani, S.O. Osisanya, A. Saasen, Modeling and Experimental Study of CO_2 Corrosion on Carbon Steel Atelevated Pressure and Temperature, J. Nat. Gas Sci. Eng, 27 (2015),pp, 1620–1629.
28. Yoichi UTANOHARA, Yukinori NAGAYA, Akira NAKAMURA, Michio MURASE, Koichi KAMAHORI. Correlation Between Flow Accelerated Corrosion and Wall Shear Stress Downstream from an Orifice, Journal of Power and Energy Systems, 7(2013), pp.138-147.
29. J.A. Wharton, R.J.K. Wood, Influence of Flow Conditions on the Corrosion of AISI 304L Stainless Steel, Wear, 256(2004), pp. 525-536.
30. Wei Li, B.F.M. Pots, Bruce Brown, Kok Eng Kee, Srdjan Nesic, A Direct Measurement of Wall Shear Stress in Multiphase Flow—Is it an Important Parameter in CO_2 Corrosion of Carbon Steel Pipelines?, Corrosion Science, 110(2016), pp.35-45.
31. Wei Li, Yao Xiong, Bruce Brown, Kok Eng Kee, Srdjan Nesic, Measurement of Wall Shear Stress in Multiphase Flow and Its Effect on Protective $FeCO_3$ Corrosion Product Layer Removal. Corrosion, 5922(2015), pp.1-15.
32. Fenyvesi Bence, Horváth Csaba, Investigation on the Nonconstant Behavior of a Vortex Flow Meter with Narrow Gauge Pipe via Conducting Measurements and Numerical Simulations, Periodica Polytechnica Mechanical Engineering, 61 (2017), pp. 247-254.
33. A. Bakker, L.M. Oshinowo, Modelling of Turbulence in Stirred Vessels Using Large Eddy Simulation, Chemical Engineering Research and Design, 82(2004), pp. 169-1178.
34. M.J. Thorsen, S. Saevik, C.M. Laren, Fatigue Damage from Time Domain Simulation of Combined In-line and Cross-flow Vortex-induced Vibrations, Marine Structures, 41(2015), pp. 200-222.
35. Y. S. Lee, S. H. Lee, K. M. Hwang, Cause Analysis of Flow Accelerated Corrosion and Erosion-Corrosion Cases in Korea Nuclear Power Plants, Corrosion Science and Technology, 15(2016), pp.182-188.